



Numerical simulation of ultrasonic enhancement on mass transfer in liquid–solid reaction by a new computational model



Qingbin Jiao^{a,b}, Bayanheshig^{a,*}, Xin Tan^a, Jiwei Zhu^a

^a National Engineering Research Center for Diffraction Gratings Manufacturing and Application, Changchun Institute of Optics, Fine Mechanics and Physics, Chinese Academy of Sciences, Dong Nanhu Road 3888, Changchun 130033, Jilin, China

^b University of Chinese Academy of Sciences, No. 19A Yuquan Road, Beijing 100049, China

ARTICLE INFO

Article history:

Received 19 April 2013

Received in revised form 4 September 2013

Accepted 4 September 2013

Available online 12 September 2013

Keywords:

Mass transfer coefficient

Numerical simulation

Ultrasonic enhancement

Liquid–solid reaction

ABSTRACT

Mass transfer coefficient is an important parameter in the process of mass transfer. It can reflect the degree of enhancement of mass transfer process in liquid–solid reaction and in non-reactive systems like dissolution and leaching, and further verify the issues by experiments in the reaction process. In the present paper, a new computational model quantitatively solving ultrasonic enhancement on mass transfer coefficient in liquid–solid reaction is established, and the mass transfer coefficient on silicon surface with a transducer at frequencies of 40 kHz, 60 kHz, 80 kHz and 100 kHz has been numerically simulated. The simulation results indicate that mass transfer coefficient increases with the increasing of ultrasound power, and the maximum value of mass transfer coefficient is 1.467×10^{-4} m/s at 60 kHz and the minimum is 1.310×10^{-4} m/s at 80 kHz in the condition when ultrasound power is 50 W (the mass transfer coefficient is 2.384×10^{-5} m/s without ultrasound). The extrinsic factors such as temperature and transducer diameter and distance between reactor and ultrasound source also influence the mass transfer coefficient on silicon surface. Mass transfer coefficient increases with the increasing temperature, with the decreasing distance between silicon and central position, with the decreasing of transducer diameter, and with the decreasing of distance between reactor and ultrasound source at the same ultrasonic power and frequency. The simulation results indicate that the computational model can quantitatively solve the ultrasonic enhancement on mass transfer coefficient.

© 2013 Elsevier B.V. All rights reserved.

1. Introduction

During the liquid–solid reaction, the interventions of ultrasound can achieve the goal of process intensification by the means of improving the chemical reaction rate effectively and increasing the chemical yield [1–3]. As an important parameter to describe the mass transfer, mass transfer coefficient can reflect the degree of enhancement on mass transfer process in liquid–solid reaction and in non-reactive systems like dissolution and leaching [4–10], and further verify the issues by experiments in the reaction process due to direct numerical relationship between it and chemical reaction rate and conversion rate [11]. So it is an important thing to solve mass transfer coefficient quantitatively.

The ultrasonic enhancement in chemical reaction is a result of both stable and transient cavitation bubbles. Two competing theories exist to explain the chemical effects due to cavitation: the electrical theory [12–14] and the hot-spot theory [15,16]. However, all these theories not only focus on the qualitative analysis of ultrasonic enhancement on mass transfer, but also fail to give a mathe-

matical method to solve that quantitatively. So the relation between mass transfer coefficient and parameters of ultrasonic field is unknown according to the theories which have been mentioned above.

The ultrasonic field could change the distribution of liquid velocity [17–23]. According to the mass transfer differential equation [24], the variation of liquid velocity could change the distribution of solution concentration, but the study of the change of distribution of solution concentration with the liquid velocity under ultrasound has not been reported in the literature. In the present paper, we put forward a new computational model to solve mass transfer coefficient quantitatively, which is including the study of the change of distribution of the liquid velocity under ultrasound effect, and the mathematical relationship between mass transfer coefficient and the distribution of solution concentration affected by liquid velocity. The relation between mass transfer coefficient and parameters of ultrasound is discussed. The effects of other factors like the different distance between silicon and central position, the transducer diameter, the distance between reactor and transducer, the placement of silicon to the mass transfer coefficient are also discussed.

* Corresponding author. Tel.: +86 13578689228.

E-mail address: bayin888@sina.com (Bayanheshig).

2. Computational model

2.1. Acoustic pressure field

The time harmonic wave equation (inhomogeneous Helmholtz equation) in media can be ascribed as:

$$\nabla \cdot \left[-\frac{1}{\rho_c} \nabla p \right] - \frac{\omega^2}{\rho_c c_c^2} p = 0 \quad (1)$$

where p represents acoustic pressure. The angular frequency ω is defined as $\omega = 2\pi f$, where f is the ultrasound frequency.

The absorption coefficient is expressed by the complex density ρ_c and sound speed c_c :

$$\rho_c = \frac{Z_c k}{\omega}, \quad c_c = \frac{\omega}{k_s}$$

The complex wave number k_s and the impedance Z_c are expressed as follows:

$$k_s = \frac{\omega}{c_s} - i\alpha, \quad Z_c = \rho_0 c_s$$

where α is the absorption coefficient, c_s and ρ_0 denote sound speed in the media and density of the media respectively.

The model has been established on the basis of the liquid–solid reaction between monocrystalline silicon and KOH solution under the ultrasound effect. The calculations have been performed in a sonochemical reactor with 100 mm in height and 150 mm in width filled with water. The sonochemical reactor was made from stainless steel. A transducer operated at 40 kHz, 60 kHz, 80 kHz and 100 kHz is mounted at the bottom of reactor center with diameter of 60 mm. A reactor with 78 mm in height and 100 mm in width filled with KOH solution whose mass fraction is 10% and a piece of silicon wafer with 60 mm in diameter and 1 mm in thickness was placed in the sonochemical reactor, which was made from quartz glass with 2 mm in thickness. The ambient temperature T is equal to 293 K. On the basis of considering the cavitation bubbles effect, the absorption coefficient should be 5 (1/m) in pressure field [25]. The schematic diagram of geometric structure is shown in Fig. 1. To save the calculation time and memory, the silicon and the quartz glass reactor were placed in form of mirror symmetry.

The impedance boundary was utilized to specify the boundary condition of water–air, water–stainless steel, water–quartz glass, quartz glass–air, KOH solution–air, KOH solution–quartz, and KOH solution–silicon wafer interfaces. The impedance boundary condition is written as:

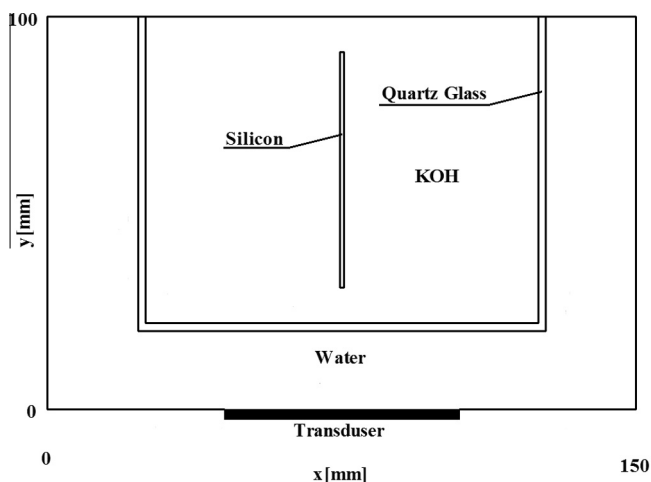


Fig. 1. The schematic diagram of geometric structure.

$$\mathbf{n} \cdot \left(-\frac{1}{\rho_c} \nabla p \right) = \frac{i\omega p}{Z_e} \quad (2)$$

where $Z_e = \rho_e c_e$ is the acoustic input impedance of the external domain (ρ_e and c_e is the density and sound speed of the external domain) and \mathbf{n} is unit normal vector against wall. The density and sound velocity of medium is shown in Table 1.

For the transducer, the boundary was set as acoustic pressure. Initial value of acoustic pressure in water, quartz glass, silicon and KOH solution was set as 0. The calculations were carried out by COMSOL Multiphysics 3.5. The calculation area consists of about 145,330 elements and in calculation the degrees of freedom is about 371,295.

2.2. The flow field

The flow field was calculated by two equations, the momentum transport equation [27–32]:

$$-\nabla \cdot \left(-p\mathbf{I} + \mu(\nabla \mathbf{u} + (\nabla \mathbf{u})^T) \right) = \mathbf{F} \quad (3)$$

and the continuity equation:

$$\nabla \cdot \mathbf{u} = 0 \quad (4)$$

where \mathbf{I} is the unit matrix, \mathbf{u} , μ and p are the liquid velocity, liquid viscosity and pressure in liquid respectively. \mathbf{F} represents the force per unit volume that causes streaming. Superscript T denotes the transpose matrix. The equation presumes constant density of the liquid throughout the reactor. During the calculation of flow field, the volume force is expressed by Eq. (5) [33–35]

$$\mathbf{F} = \frac{2\alpha}{\rho_0 c_0^2} |p|^2 \quad (5)$$

The no slip wall was used as the boundary condition to specify silicon surface, quartz glass surface and transducer surface as a stationary solid wall. This boundary condition is prescribed as:

$$\mathbf{u} = 0 \quad (6)$$

According to the formula [36]:

$$\left[\eta_{\text{sol}} / \eta_{\text{H}_2\text{O}} = 2 \right]_{c_2 < 30\%}$$

The viscosity of KOH is equal to 2.548×10^{-3} (Pa s). The initial liquid velocity in KOH solution was set as 0 and the thermal convection effect has not been taken into account. The calculations were carried out by COMSOL Multiphysics 3.5. The calculation area consists of about 45,680 elements and in calculation the degrees of freedom is about 150,693.

2.3. The species transport field

The species transport field was calculated by two equations, the mass transfer differential equation:

$$\frac{\partial c}{\partial t} + \nabla \cdot (-D\nabla c) + \mathbf{u} \cdot \nabla c = 0 \quad (7)$$

and the mass flux equation:

Table 1
The density and sound velocity of medium [26].

Medium	Density (kg/m ³)	Sound velocity (m/s)
Water	1000	1500
Stainless steel	7800	6010
Quartz glass	2700	5760
Monocrystalline silicon	2330	7140
10% KOH solution	1054	1500

$$N = -D\nabla c + \mathbf{u}c \quad (8)$$

where D , c , N are the diffusion coefficient, the molarity, chemical reaction rate and total mass flux of constituent A respectively. \mathbf{u} is the velocity of liquid in reactor.

The no flux was used as the boundary condition to specify that there is no mass flux on quartz glass surface and KOH solution–air interface. This boundary condition is prescribed as:

$$-\mathbf{n} \cdot \mathbf{N} = 0 \quad (9)$$

The flux has been used to specify that there is mass flux on silicon surface. This boundary condition is prescribed as:

$$-\mathbf{n} \cdot \mathbf{N} = N_0 \quad (10)$$

$$N_0 = q \quad (11)$$

where N_0 is the mass flux on silicon surface, q is the surface reaction rate whose unit is mol/m² s.

The reaction between silicon and KOH solution is a 1/4 order irreversible reaction [37], so we could determine that $q = k(c_{AS})^{0.25}$, $k = k_0 \exp(-E_a/RT)$ [38,39], where c_{AS} is the surface concentration of KOH solution on silicon surface, k is the rate constant. In order to confirm k_0 and E_a under the sonicated conditions of frequencies at 40 kHz, 60 kHz, 80 kHz and 100 kHz, we design a series of experiments on the basis of fundamental method [36]. Firstly, we study the relationship between etching rate and ultrasound frequency on silicon (100) wafer. The range of temperature is 20–60 °C, the mole concentration of KOH solution is 1882 mol/m³ (mass fraction is 10%), the ultrasound frequencies are 40 kHz, 60 kHz, 80 kHz and 100 kHz and the ultrasound power are 10 W, 20 W, 30 W, 40 W and 50 W respectively. The silicon wafer is covered with a passivation layer (SiO₂) with periodic pattern by using standard photolithographic process. The activation energy E_a and frequency factor R_0 under the sonicated conditions of frequencies at 40 kHz, 60 kHz, 80 kHz and 100 kHz are calculated by using the relationship between etching rate and temperature $R = R_0 \exp(-E_a/kT)$ [37,38,40], and analyzing the data of etching rate measured in experiment through using numerical method. The amount of substance of silicon consumed in unit time and unit area is equal to $dn_{Si} = (\rho_{Si} \cdot R \cdot dt \cdot ds)/M_{Si}$, we know that the surface thickness is about equal to the summation of thickness of several atoms, and the etching rate of Si–KOH is about several nanometers per second, so we get that if the time interval dt is a smaller value, the body reaction can be seen as a surface reaction. Then the surface reaction rate q_{Si} can be written as $q_{Si} = dn_{Si}/(dt \cdot ds) = \rho_{Si} \cdot R/M_{Si}$. According to reactive equation $\text{Si} + 2\text{OH}^- \rightarrow 2\text{H}_2$, we can get that the amount of substance of OH⁻ $dn_{\text{OH}^-} = 2dn_{\text{Si}}$, so the surface reaction rate of OH⁻ $q = dn_{\text{OH}^-}/(dt \cdot ds) = 2dn_{\text{Si}}/(dt \cdot ds) = 2\rho_{\text{Si}} \cdot R/M_{\text{Si}} = k(c_A)^{0.25}$. We can get the Arrhenius constant k_0 under the sonicated conditions of frequencies at 40 kHz, 60 kHz, 80 kHz and 100 kHz through calculating, and the results are shown in Table 2.

The diffusion coefficient $D = 2.711 \times 10^{-9}$ (m²/s) [41], and the molarity of KOH solution is equal to 1882 (mol/m³). The initial molarity of KOH solution was set as 1882 (mol/m³). The calculations were carried out by COMSOL Multiphysics 3.5. The calculation area consists of about 32,680 elements and in calculation the degrees of freedom is about 110,693.

Firstly, the acoustic pressure distributions by numerical simulation were used to obtain the volume force using volume force equation and the liquid velocity distribution was calculated by using the momentum transport equation and the concentration distribution were calculated by using the mass transfer differential equation. Secondly, the surface molarity c_{AS} and the concentration gradient dc/dx perpendicular to the silicon surface were further calculated by using the function of post-processing of COMSOL. Finally, the mass transfer coefficient k_c is calculated by using Eq. (12)

[24,42], where c_A is the main molarity. The computational domain sketch showing distribution of elements can be seen in Fig. 2:

$$k_c = \frac{-D \frac{dc_A}{dx} \big|_{x=0}}{(c_{AS} - c_A)} \quad (12)$$

3. Results and discussion

3.1. Effect of essential factors of ultrasonic field

The essential factors having enhancement on mass transfer coefficient are frequencies and power of ultrasonic field. For the convenience of discussion, a parameter named ultrasound-enhancement coefficient is defined to characterize the degree of ultrasonic enhancement on mass transfer, which is the ratio of mass transfer coefficient with ultrasound divided by that without ultrasound.

Fig. 3 shows the simulation results of mass transfer coefficient to ultrasonic field with frequency at 40 kHz and ultrasound power at the range from 10 W to 50 W. The results indicate that mass transfer coefficient on silicon surface in reactor with ultrasound is higher than that without ultrasound, and mass transfer coefficient increases with the increasing ultrasound power. Similar results are also suitable for other frequencies discussed in our paper. However, mass transfer coefficient does not increase with the increasing frequency, the simulation results are shown in Fig. 4. In the condition of the same ultrasound power at 50 W, the maximum value of ultrasound-enhancement coefficient is at 60 kHz and the minimum value is at 80 kHz. The maximum value is equal to 6.15 and the minimum value is equal to 5.49. The ultrasound generated flow could improve the mixing process [43,44], which means that the process of convective mass transfer can be enhanced meanwhile. During the process of simulation, we found that the liquid velocity declines in order of 60 kHz, 100 kHz, 40 kHz and 80 kHz, which causes the process of convective mass transfer by convection becoming faster at 60 kHz and slower at 80 kHz. So the enhancement effect to mass transfer coefficient is higher at 60 kHz and lower at 80 kHz.

To the liquid–solid reaction A (fluid) + bB (solid) → fluid and solid products, the Shrinking-Core Model [11] can be described as $-\frac{1}{S} \frac{dn_B}{dt} = bk_c(C_A - C_{AS})$, where $n_B = \frac{m_B}{M_B} = \frac{\rho_B V_B}{M_B}$, k_c , C_A and C_{AS} is the mass transfer coefficient, the main molarity and the surface molarity respectively. We know that $V_B = S \cdot L$, and $n_B = \frac{\rho_B S L}{M_B}$, where S , ρ_B and M_B are all constants. To the physical truth, only the surface reaction between silicon upper surface and KOH solution exists during the reaction process and other surfaces do not participate in the surface reaction. We can get $dn_B = \frac{\rho_B S}{M_B} dL$ and $-\frac{1}{S} \frac{dn_B}{dt} = -\frac{\rho_B}{M_B} \frac{dL}{dt} = bk_c(C_A - C_{AS})$, further $\frac{dL}{dt} = -\frac{bM_B}{\rho_B} k_c(C_A - C_{AS})$. To the discussion in our paper, $\frac{dL}{dt}$ is the etching rate R in process of the silicon wet etching and $R = -\frac{bM_B}{\rho_B} k_c(C_A - C_{AS})$.

According to the reaction equation: $2\text{OH}^- + \text{Si} \rightleftharpoons \text{SiO}_2(\text{OH})_2^- + 2\text{H}_2 \uparrow$, we can get $b = 0.5$. To the silicon, the molar mass M_B and the density ρ_B is 28×10^{-3} (kg/mol) and 2330 (kg/m³) respectively. Putting k_c , C_A and C_{AS} calculated by the computational model established in our paper in the equation $R = -\frac{bM_B}{\rho_B} k_c(C_A - C_{AS})$, we can get the numerical solutions of the etching rate. Comparing the simulated results with the experimental results, the accuracy of numerical solutions calculated by the computational model established in our paper can be proved indirectly.

3.2. Effect of extrinsic factors

In Section 3.1, we discuss the enhancement effect of essential factors to mass transfer coefficient quantitatively and deeply. In

Table 2
The activation energy and Arrhenius constant.

Frequency (kHz)	Ultrasound power (W)	Activation energy (E_a) (Ev)	Arrhenius constant (k_0) ($\text{mol}^{0.75}/(\text{m}^{1.25} \text{ s})$)
40	10	0.465	495
	20	0.464	644
	30	0.461	753
	40	0.459	892
	50	0.458	1051
60	10	0.436	253
	20	0.434	308
	30	0.433	409
	40	0.431	407
	50	0.429	399
80	10	0.472	462
	20	0.470	622
	30	0.469	791
	40	0.466	942
	50	0.464	983
100	10	0.460	404
	20	0.457	478
	30	0.454	553
	40	0.451	639
	50	0.448	677
Without ultrasound		0.595	2480

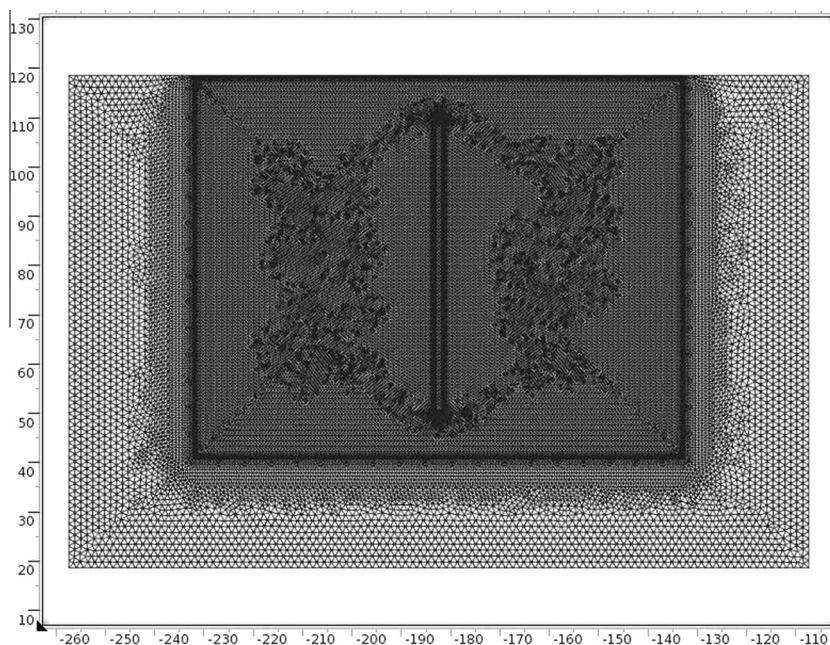


Fig. 2. The computational domain sketch showing distribution of elements.

the practical application, extrinsic factors such as temperature, distance between silicon and central position, different placements of silicon wafer, the transducer diameter and the distance between reactor and ultrasound source are also influential to the ultrasonic enhancement on mass transfer coefficient. Aiming at ultrasonic field with frequency at 40 kHz, and ultrasound power at the range from 10 W to 50 W, we discuss the effects of temperature, distance between silicon and central position, different placement of silicon, transducer diameter and distance between reactor and ultrasound source in Section 3.2.1–3.2.5 respectively. In Section 3.2.1–3.2.5, the transducer diameter is 60 mm.

3.2.1. Effect of the temperature

Fig. 5 shows the simulation result of mass transfer coefficient with different temperatures. The range of temperature is 293–

353 K. As shown, the mass transfer coefficient increases with the increasing temperature. The viscosity of KOH solution decreases with the increasing temperature, which could cause the velocity of solution increasing. Meanwhile, the surface reaction rate increases with the increasing temperature. The increasing velocity of solution and surface reaction rate could cause the concentration gradient dc/dx on silicon surface increasing. When temperature is increasing, the diffusion coefficient D is increasing. The increasing concentration gradient and diffusion coefficient could cause the ultrasonic enhancement on mass transfer coefficient increasing.

3.2.2. Effect of the distance between silicon and central position

Fig. 6 shows the simulation result of mass transfer coefficient with distance between silicon and central position. The mass transfer coefficient decreases with the increasing distance between sil-

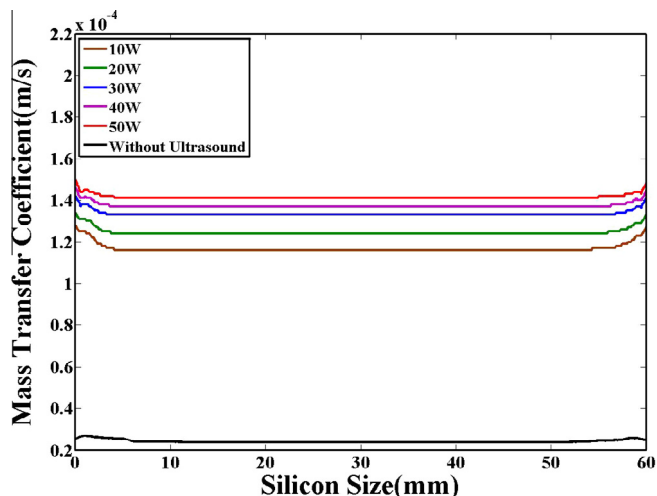


Fig. 3. The comparison chart of mass transport coefficient with ultrasound of frequency at 40 kHz and without ultrasound.

icon and central position. According to the simulation results of velocity distribution, the liquid velocity decreases with the increasing distance and further, the enhancement on the process of convective mass transfer becomes slower, which causes the ultrasonic enhancement on mass transfer coefficient decreasing.

3.2.3. Effect of different placement of silicon

Fig. 7 shows the simulation result of mass transfer coefficient with different placement of silicon. The maximum value of ultrasound-enhancement coefficient is 5.92 when setting silicon vertically, but the maximum value of ultrasound-enhancement coefficient is 5.53 when setting silicon horizontally. The mass transfer coefficient when we set silicon vertically is higher than that when setting silicon horizontally. The results indicate that setting silicon horizontally is not conducive to the process of convective mass transfer and the acquisition of higher ultrasound-enhancement coefficient. Setting silicon horizontally is not beneficial to improving the liquid velocity. Therefore, the process of convective mass transfer becomes slower, and the enhancement effect to mass transfer decreasing.

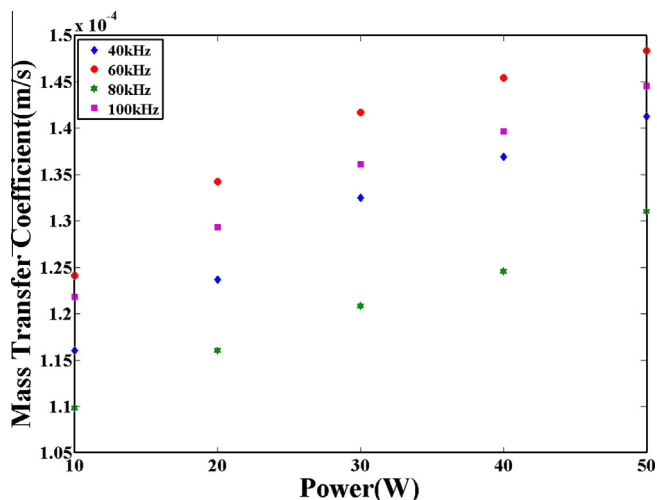


Fig. 4. The comparison chart of mass transport coefficient influenced with different frequencies.

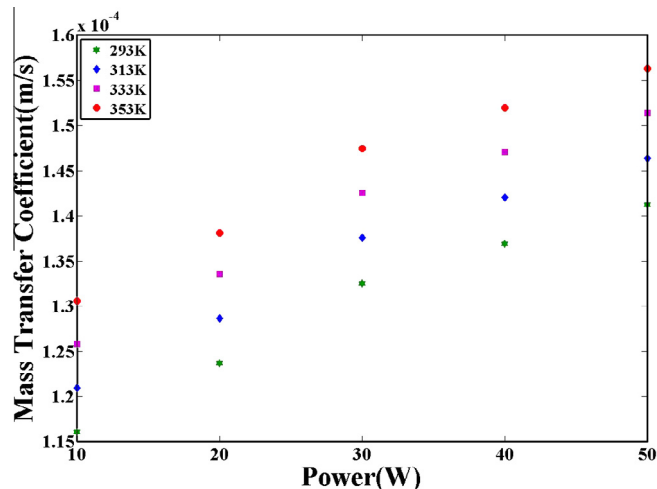


Fig. 5. The comparison chart of mass transfer coefficient to different temperature.

3.2.4. Effect of transducer diameter

Fig. 8 shows the simulation result of mass transfer coefficient with different transducer diameters. The mass transfer coefficient decreases with the increasing transducer diameter. The liquid velocity decreases with the increasing transducer diameters [10] and further, the process of convective mass transfer becomes slower, which causes the enhancement effect to mass transfer coefficient decreasing.

3.2.5. The effect of distance between the reactor and ultrasound source

Fig. 9 shows the simulation result of mass transfer coefficient with different distances between the reactor and ultrasound source. The maximum ultrasound-enhancement coefficients are 5.92, 5.69, 5.40 and 5.14 respectively. Thus, the maximum ultrasound-enhancement coefficient has the great value against distance between the reactor and ultrasound source, and the mass transfer coefficient decreases with the increasing of distance between the reactor and ultrasound source. The liquid velocity decreases with the increasing different distances between the reactor and ultrasound source and further, the process of convective mass transfer becomes slower, which causes the enhancement effect to mass transfer coefficient decreasing.

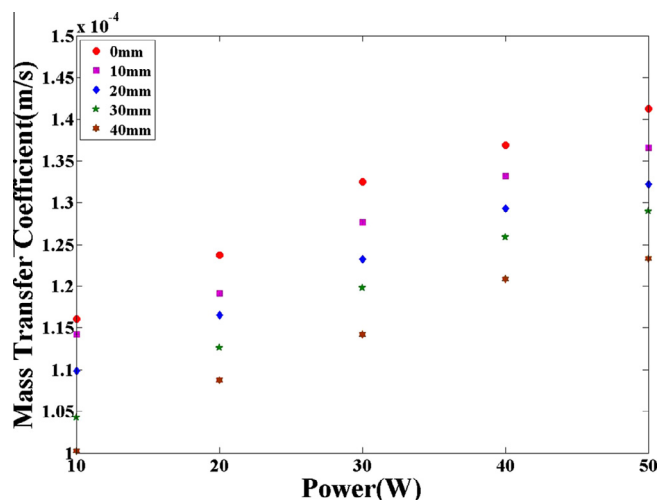


Fig. 6. The comparison chart of mass transfer coefficient to different distance between silicon and the middle position.

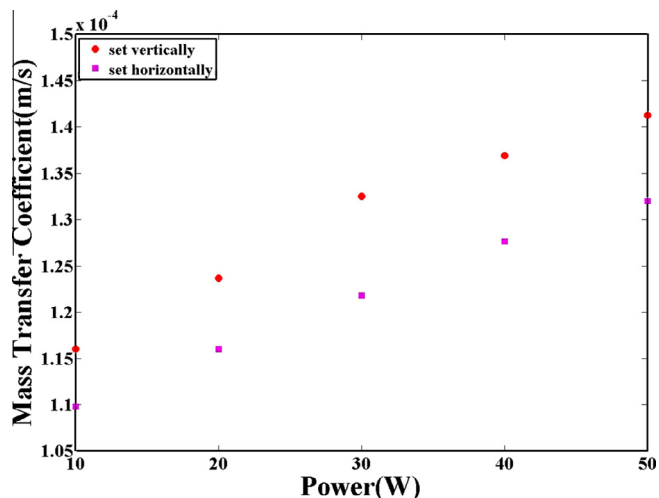


Fig. 7. The comparison chart of mass transfer coefficient to different placement of silicon.

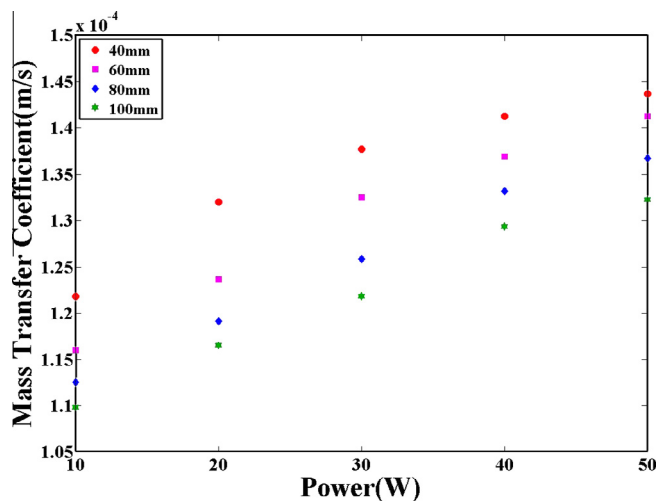


Fig. 8. The trend of mass transfer coefficient to the transducer diameter.

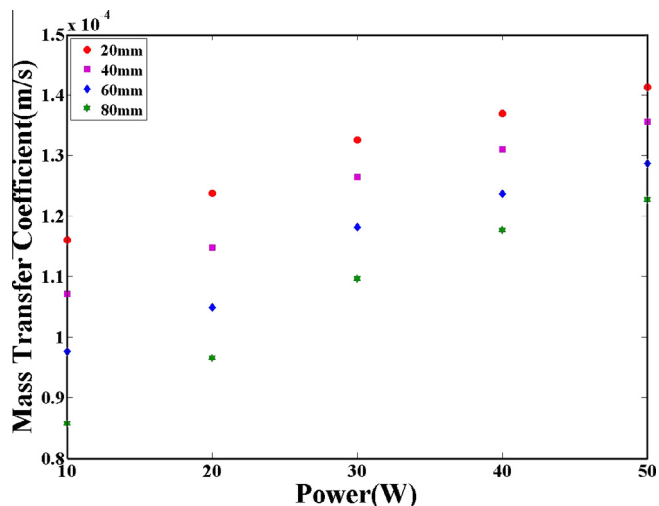


Fig. 9. The trend of mass transfer coefficient to the distance between the reactor and ultrasound source.

4. Conclusion

A new computational model quantitatively solving mass transfer coefficient of liquid–solid reaction under ultrasonic enhancement is established, and the mass transfer coefficient has been investigated by numerical simulation. The enhancement effect of essential factors including frequencies and ultrasound power of ultrasound and extrinsic factors such as different placements of silicon wafer, the size of transducer and the distance between reactor and ultrasound source have also been investigated. The results indicate that: (a) mass transfer coefficient increases with the increasing of ultrasound power, (b) mass transfer coefficient increases with the increasing of temperature, (c) mass transfer coefficient increases with the decreasing distance between silicon and central position, and there is the maximum value of enhancement effect at the central position of model, (d) mass transfer coefficient when set silicon vertically is higher than that when set silicon horizontally, (e) mass transfer coefficient increases with the decreasing of transducer diameter, and (f) mass transfer coefficient increases with the decreasing of distance between reactor and ultrasound source.

Acknowledgment

This work is supported by the Project developing key scientific instrument and equipment of China (2011YQ120023).

References

- [1] Vijayanand Moholkar, Marijn C.G. Warmoeskerken, Mechanism of mass-transfer enhancement in textiles by ultrasound, *AIChE J.* 50 (2004) 58–64.
- [2] Cunshan Zhou, Haile Ma, Ultrasonic degradation of polysaccharide from a red algae (*Porphyra yezoensis*), *J. Agric. Food Chem.* 54 (2006) 2223–2228.
- [3] V.S. Moholkar, M.M.C.G. Warmoeskerken, Investigations in mass transfer enhancement in textiles with ultrasound, *Chem. Eng. Sci.* 59 (2004) 299–311.
- [4] Cass T. Miller, Michele M. Poirier-McNeil, Alex S. Mayer, Dissolution of trapped nonaqueous phase liquids: mass transfer characteristics, *Water Resour. Res.* 26 (1990) 2783–2796.
- [5] Susan E. Powers, Linda M. Abriola, Walter J. Weber Jr., An experimental investigation of nonaqueous phase liquid dissolution in saturated subsurface systems: steady state mass transfer rates, *Water Resour. Res.* 28 (1992) 2691–2705.
- [6] A.W. Nienow, Dissolution mass transfer in a turbine agitated baffled vessel, *Can. J. Chem. Eng.* 47 (1969) 248–258.
- [7] Alex S. Mayer, Cass T. Miller, The influence of mass transfer characteristics and porous media heterogeneity on nonaqueous phase dissolution, *Water Resour. Res.* 32 (1996) 1551–1567.
- [8] Wolfgang Dreybrodt, Dieter Buhmann, A mass transfer model for dissolution and precipitation of calcite from solutions in turbulent motion, *Chem. Geol.* 90 (1991) 107–122.
- [9] G.H. Brimhall, Lithologic determination of mass transfer mechanisms of multiple-stage porphyry mineralization at Butte, Montana; vein formation by hypogene leaching and enrichment of potassium-silicate protore, *Econ. Geol.* 74 (1979) 556–589.
- [10] C. Vu, K.N. Han, Effect of system geometry on the leaching behavior of cobalt metal: mass transfer controlling case, *Metall. Trans. B* 10 (1979) 57–62.
- [11] Octave Levenspiel, *Chemical Reaction Engineering*, third ed., John Wiley & Sons, New York, 1999.
- [12] M.A. Margulis, Sonoluminescence and sonochemical reactions in cavitation fields. A review, *Ultrasonics* 23 (1985) 157–169.
- [13] M.A. Margulis, Fundamental aspects of sonochemistry, *Ultrasonics* 30 (1992) 152–155.
- [14] M.A. Margulis, Fundamental problems of sonochemistry and cavitation, *Ultrason. Sonochem.* 1 (1994) 87–90.
- [15] Kenneth S. Suslick, David A. Hammerton, Raymond E. Cline Jr., The sonochemical hot spot, *J. Am. Chem. Soc.* 108 (1986) 5641–5642.
- [16] Ying Chongfu, A.N. Yu, Distributions of the high temperature and the high pressure inside a single acoustically driven bubble, *Sci. China Ser. A* 45 (2002) 926–936.
- [17] Zheng Xu, Keiji Yasuda, Shinobu Koda, Numerical simulation of liquid velocity distribution in a sonochemical reactor, *Ultrason. Sonochem.* 20 (2013) 452–459.
- [18] M. Chouvellon, A. Largillier, T. Fournel, P. Boldo, Y. Gonthier, Velocity study in an ultrasonic reactor, *Ultrason. Sonochem.* 7 (2000) 207–211.
- [19] Yoshihiro Kojima, Yoshiyuki Asakura, Genki Sugiyama, Shinobu Koda, The effects of acoustic flow and mechanical flow on the sonochemical efficiency in a rectangular sonochemical reactor, *Ultrason. Sonochem.* 17 (2010) 978–984.

- [20] A. Mandroyan, R. Viennet, Y. Bailly, M.L. Doche, J.Y. Hihn, Modification of the ultrasound induced activity by the presence of an electrode in a sonoreactor working at two low frequencies (20 and 40 kHz). Part I: Active zone visualization by laser tomography, *Ultrason. Sonochem.* 16 (2009) 88–97.
- [21] A. Mandroyan, M.L. Doche, J.Y. Hihn, R. Viennet, Y. Bailly, L. Simonin, Modification of the ultrasound induced activity by the presence of an electrode in a sonoreactor working at two low frequencies (20 and 40 kHz). Part II: Mapping flow velocities by particle image velocimetry (PIV), *Ultrason. Sonochem.* 16 (2009) 97–104.
- [22] Y. Kojima, Y. Asakura, G. Sugiyama, S. Koda, The effects of acoustic flow and mechanical flow on the sono-chemical efficiency in a rectangular sonochemical reactor, *Ultrason. Sonochem.* 17 (2010) 978–984.
- [23] F.J. Trujillo, K. Knoerzer, A computational modeling approach of the jet-like acoustic streaming and heat generation induced by low frequency high power ultrasonic horn reactors, *Ultrason. Sonochem.* 18 (2011) 1263–1273.
- [24] James R. Welty, Charles E. Wicks, Robert E. Wilson, Gregory L. Rorrer, *Fundamentals of Momentum, Heat and Mass Transfer*, fifth ed., John Wiley & Sons, New York, 2000.
- [25] K. Yasui, T. Kozuka, T. Tuziuti, A. Towata, Y. Iida, J. King, P. Macey, FEM calculation of an acoustic field in a sonochemical reactor, *Ultrason. Sonochem.* 14 (2007) 605–614.
- [26] Paul Mataboni, Edward Schreiber, Method of pulse transmission measurements for determining sound velocities, *J. Geophys. Res.* 72 (1967) 5160–5163.
- [27] W.L. Nyborg, Acoustic streaming due to attenuated plane waves, *J. Acoust. Soc. Am.* 25 (1953) 68–75.
- [28] L. Rayleigh, *Theory of Sound*, Dover Publications, New York, 1896.
- [29] P.J. Westervelt, The theory of steady rotational flow generated by a sound field, *J. Acoust. Soc. Am.* 25 (1953) 60–67.
- [30] L.K. Zaremba, Acoustic streaming, in: L.D. Rozenberg (Ed.), *High Intensity Ultrasonic Fields*, Plenum Press, New York, London, 1971, pp. 141–169.
- [31] W.M. Kays, M.E. Crawford, *Convective Heat and Mass Transfer*, third ed., McGraw-Hill, Inc., New York, 1993.
- [32] Herbert Oertel, *Prandtl-Essentials of Fluid Mechanics*, third ed., Springer, New York, 2010.
- [33] J. Wu, G. Du, Acoustic streaming generated by a focused Gaussian beam and finite amplitude tonebursts, *Ultrasound Med. Biol.* 19 (1993) 167–176.
- [34] S.I. Aanonsen, T. Barkve, J.N. Tjøtta, S. Tjøtta, Distortion and harmonic generation in the nearfield of a finite amplitude sound beam, *J. Acoust. Soc. Am.* 75 (1984) 749–768.
- [35] K.R. Nightingale, G.E. Trahey, A finite element model for simulating acoustic streaming in cystic breast lesions with experimental validation, *IEEE Trans. Ultrason. Ferr.* 47 (2000) 201–215.
- [36] D.Q. Kern, *Process of Heat Transfer*, McGraw-Hill, New York, 1950.
- [37] H. Seidel, L. Csepregi, A. Heuberger, H. Baumgartel, Anisotropic etching of crystalline silicon in alkaline solutions: I. Orientation dependence and behavior of passivation, *J. Electrochem. Soc.* 137 (1990) 3612–3626.
- [38] Jue Peng, Chen Chao, Jiyuan Dai, Helen L.W. Chan, Haosu Luo, Micro-patterning of 0.70Pb (Mg_{1/3}Nb_{2/3})O₃-0.30PbTiO₃ single crystals by ultrasonic wet chemical etching, *Mater. Lett.* 62 (2008) 3127–3130.
- [39] J.W. Chen, Walter M. Kalback, Effect of ultrasound on chemical reaction rate, *Ind. Eng. Chem. Fundam.* 6 (1967) 175–178.
- [40] P.M. Zavrocky, T. Earles, N.L. Pokrovskiy, J.A. Green, B.E. Burns, Fabrication of vertical sidewalls by anisotropic etching of silicon (1 0 0) wafer, *J. Electrochem. Soc.* 141 (1994) 3182–3188.
- [41] J.-F. Dufrière, O. Bernard, P. Turq, Transport equations for concentrated electrolyte solutions: reference frame, mutual diffusion, *J. Chem. Phys.* 116 (2002) 2085–2097.
- [42] Hans Dieter Baehr, Karl Stephan, *Heat and Mass Transfer*, second ed., Springer, Berlin, 2006.
- [43] Nilesh P. Vichare, Parag R. Gogate, Vishwas Y. Dindore, Aniruddha B. Pandit, Mixing time analysis of a sonochemical reactor, *Ultrason. Sonochem.* 8 (2001) 23–33.
- [44] Parag R. Gogate, Vinayak S. Sutkar, Aniruddha B. Pandit, Sonochemical reactors: important design and scale up considerations with a special emphasis on heterogeneous systems, *Chem. Eng. J.* 166 (2011) 1066–1082.